Proc. Int. Conf. on Monitoring, Prediction and Mitigation of Water-Related Disasters,
Disaster Prevention Research Institute, Kyoto Univ. (2005)

Storm Surge and Tsunami Simulator in Oceans and Coastal Areas

Taro Kakinuma and Takashi Tomita
Marine Environment and Engineering Department, Port and Airport Research Institute,
3-1-1 Nagase, Yokosuka, Kanagawa 239-0826, Japan

ABSTRACT: This paper describes a numerical model for storm surge and tsunami simulation considering three-dimensional characteristics of flow. The developed model, STOC (Storm surge and Tsunami simulator in Oceans and Coastal areas), consists of three parts: 1) 3D model, 2) multilevel model and 3) connection model. The 3D model is applied to a narrow area surrounded by a wider area, which is covered by the multilevel model. By adopting the 3D model locally we can economically and accurately evaluate complicated flow around coastal structures or over various topographies, which are smoothly expressed with a porous model introduced into the set of continuity and Navier-Stokes equations. STOC was applied to the 1868 Meiji-Sanriku tsunami, resulting in representation of a remarkably three-dimensional velocity around the open mouth of tsunami breakwaters as well as the total pressure including both hydrostatic and dynamic pressures on the superstructure of submerged breakwater.

1 INTRODUCTION

Seawater motion from offshore to coastal zones, which includes phenomena of various scales on both space and time, should be solved efficiently in numerical calculation. For this purpose a hybrid model, which consists of a 3D model, a multilevel model and a connection model, has been developed to simulate three-dimensional flow due to tsunamis or storm surges. By local application of the 3D model to narrower areas surrounded by wider areas which are covered by the multilevel model, we can represent three-dimensional characteristics of fluid motion around structures over steep topography economically and accurately.

The governing equations are the continuity and Navier-Stokes equations for incompressible fluids, where a porous model as presented by Sakakiyama and Kajima (1992) is adopted to describe configurations of structure and seabed smoothly. We solve this set of equations using numerical schemes based on the finite difference method by Masamura *et al*. (2001), who connected a 3D model to a hydrostatic one-layer model. In the present study we have connected the 3D model, where pressure is not assumed to be hydrostatic, to the hydrostatic but multilevel model, into which two additional models are introduced: 1) the seismic deformation model (Mansinha and Smylie, 1971) to generate tsunamis, and 2) Myers model to describe both pressure decrease and wind drag force caused on the sea surface by tropical cyclones. Applying the multilevel model to a wide area of ocean, we can represent vertical distribution of velocity in storm surges, as well as not only nonlinearity but also dispersivity of tsunamis.

The new hybrid model was applied to the 1868 Meiji-Sanriku tsunami to examine complicated flow around the tsunami breakwaters of Kamaishi Port, Japan, resulting in evaluation of total pressure including both hydrostatic and dynamic pressures on the structures.

For disaster prevention, many things are important to be stocked by individuals as well as their organizations, e.g. food, facility, commodity, knowledge, information, attitude of mind, etc. Accordingly we call this numerical calculation model “Storm surge and Tsunami simulator in Oceans and Coastal areas,” i.e., STOC.

2 NUMERICAL MODEL

2.1 Governing equations

In the numerical simulator, STOC, we solve the following set of continuity and Navier-Stokes equations, i.e.,

$$\frac{\partial \gamma_i u_i}{\partial x_i} = 0 \,, \tag{1}$$

$$\varepsilon \frac{\partial u_i}{\partial t} + \frac{\partial \gamma_j u_i u_j}{\partial x_j} + C_i = -\frac{\varepsilon}{\rho_0}\frac{\partial p}{\partial x_i} + \varepsilon \frac{\rho - \rho_0}{\rho_0} g_i + \frac{\partial}{\partial x_j}\left\{\gamma_j \nu_T \left(\frac{\partial u_i}{\partial x_j} + \frac{\partial v_j}{\partial x_i}\right)\right\}, \tag{2}$$

where x_i describes Cartesian coordinate system, (x, y, z); u_i is velocity in the direction of x_i, (u, v, w); ρ is density; ρ_0 is reference density; p is pressure; ε is porosity; γ_i is transmissivity in the direction of x_i; g_i is gravitational acceleration; ν_T is total viscosity including kinematic viscosity and eddy viscosity; C_i is Coriolis term. These porosity and transmissivity are introduced to express configurations of sea bottoms or structure faces smoothly as in the porous model presented by Sakakiyama and Kajima (1992).

We solve these governing equations using numerical schemes based on the finite difference method by Masamura *et al*. (2001), who connected a 3D model to a hydrostatic one-layer model. A spatially staggered mesh is adopted, i.e., the diffusion terms are discretized with the second-order central scheme, while the advection terms are expanded with a hybrid scheme where the first-order upwind scheme is combined with the second-order central scheme using weightings for stability. In the temporal direction a leapfrog method is utilized to stagger calculation time-steps of velocity and those of both water surface displacement and pressure.

2.2 Structure of numerical simulator, STOC

2.2.1 Multilevel model

STOC consists of three parts as shown in Fig. 1: 1) 3D model, 2) multilevel model and 3) connection model.

In wide-area calculation we use the multilevel model named STOC-ML, which solves vertically integrated continuity and Navier-Stokes equations in each level with assumption of hydrostatic pressure. Two physical models are introduced into STOC-ML: 1) the seismic deformation model (Mansinha and Smylie, 1971) to generate tsunamis due to submarine earthquakes, and 2) Myers model to describe both pressure decrease and wind drag force caused by tropical cyclones.

2.2.2 3D model

The 3D model labeled as STOC-NS is applied locally to a narrower area, where pressure is solved without assumption of hydrostatic pressure, such that we can economically and accurately evaluate complicated distribution of velocity and pressure around coastal structures over steep topography.

2.2.3 Connection model

For smooth connection between multilevel areas and 3D areas, a connection model should be applied to overlap regions, where physical variables are defined by interpolation of those in the two areas. The interpolated variables are selected among water surface elevation, velocity, momentum, pressure, eddy viscosity coefficient, etc. In the connection model we can choose between two connecting methods, i.e., two-way method and one-way method.

The two-way method solves both the multilevel model and the 3D model in an overlapping area simultaneously at each time-step to consider interaction of phenomena in the multilevel area and the 3D area. When more accuracy than speed is required in calculation, it is recommended applying this two-way method.

On the other hand, in the one-way method, we perform calculation over the whole domain throughout the target period using the multilevel model, after which we solve the 3D model with interpolated variables on outer boundaries of connection areas. Thus the results obtained by the multilevel model are reflected in the 3D calculation but the reverse is not done. This one-way method is adequate to immediate calculation, where the 3D model can run at different time-steps from those of the multilevel model, even if the 3D calculation requires much shorter intervals of time-steps corresponding to its minute meshes.

In the present calculation we use the one-way method, where interpolation is conducted for only water surface elevation. Specifically, water surface displacement inside connection areas is compensated by

$$\eta * = k\eta_{NS} + (1-k)\eta_{ML}, \tag{3}$$

where η_{NS} and η_{ML} are water surface displacements calculated at the last time-step by STOC-NS and STOC-ML, respectively. The weighting k changes gradually from 0 to 1 through the connection area from the multilevel area to the 3D area for consistency of physical variables, resulting in stability of numerical calculation. This compensated value, $\eta *$, is used in calculation at the following time-steps.

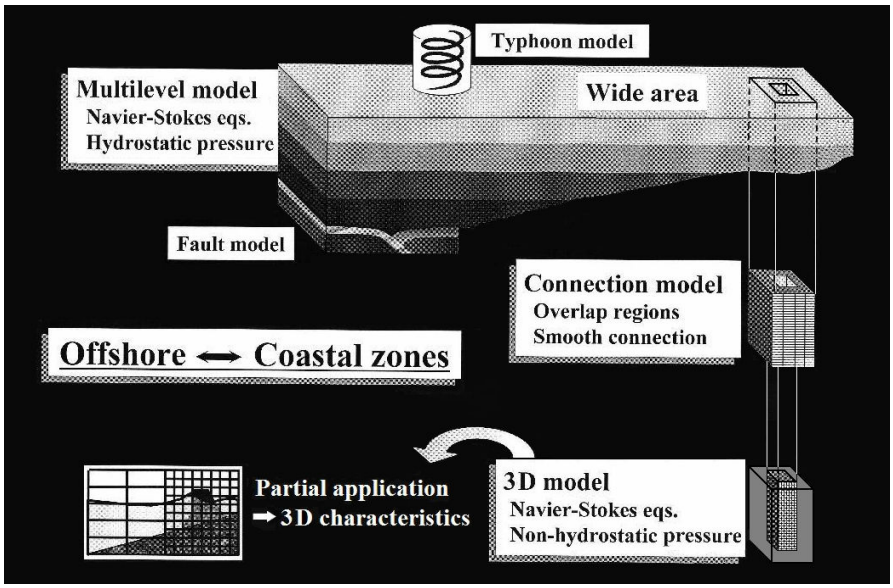

Figure 1. Diagram of STOC.

2.3 Calculation method of water surface displacement

After calculation in cells at the current time-step, we should know position of water surface at the next time-step. In STOC-NS and STOC-ML we use the vertically integrated equation of continuity, i.e.,

$$\gamma_z \frac{\partial \eta}{\partial t} + \frac{\partial}{\partial x}\int_{-h}^{\eta} \gamma_x u \, dz + \frac{\partial}{\partial y}\int_{-h}^{\eta} \gamma_y v \, dz = 0, \tag{4}$$

where η is water surface displacement and h is still water depth.

In runup or inundation regions, a *bucket-brigade* method is used, i.e., there exists water where water depth is larger than some reference value $h_{\min}$, e.g. $h_{\min} = 1.0 \times 10^{-4}$m.

3 VERIFICATION OF STOC-NS

We have confirmed accuracy of STOC by comparing its results with those of other numerical models or hydraulic experiments for various benchmark tests. Several results obtained by STOC-NS are shown here.

Figure 2(a) shows the calculation result by STOC-NS of velocity in horizontal cavity flow with a side wall sliding at a constant speed of u_0 in the positive direction of x where $y/d = 1.0$. Every calculation result in this paper has been obtained under nonslip condition on any walls and bottoms. In Fig. 2(b) we can see correspondence between the distribution along the line where $x/d = 0.5$ of velocity in the direction of x, u, obtained by STOC-NS and that given by another commercial numerical model, α-FLOW.

Figure 3 shows calculation results by STOC-NS of a drift current entailed by a wind blowing in the positive direction of x. In this problem we have theoretical solutions of water surface gradient and horizontal velocity, i.e.,

$$\frac{\partial \eta}{\partial x} = \frac{3 r f_a}{2 g h} U|U| \quad \text{and} \quad u = \frac{h r f_a}{4 K_z}\left(1 + \frac{z}{h}\right)\left(1 + \frac{3z}{h}\right) U|U|, \tag{5}$$

where η is water surface displacement; u is horizontal velocity along the line where x = 500m. In the calculation for Fig. 3, wind speed on sea surface U = 20m/s; friction coefficient on sea surface f_a = 0.0026; density ratio of atmosphere and seawater $r = 1.2 \times 10^{-3}$; kinematic eddy viscosity coefficient $K_z = 0.01\text{m}^2/\text{s}$; still water depth h = 10.1m. This benchmark test is for verification of wind-driven currents in storm-surge calculation.

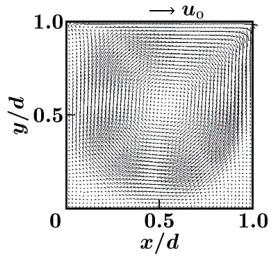

(a) Velocity vectors.

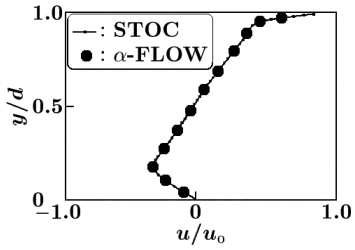

(b) Velocity in the direction of x, u (x/d = 0.5).

Figure 2. Calculation results of 2D cavity flow.

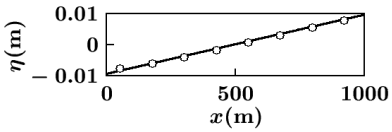

(a) Water surface elevation.

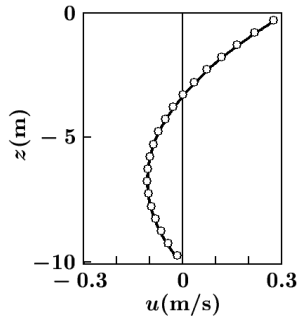

(b) Horizontal velocity (x = 500m).

Figure 3. Water surface elevation and horizontal velocity in wind-driven current: Calculation results by STOC-NS (o) in comparison with the correspondent theoretical solutions by Eq. (5) (–).

4 NUMERICAL SIMULATION

4.1 Calculation conditions

STOC can treat the whole area from offshore, where submarine earthquakes are generated, to coastal zones, which include coastal structures. In this study we apply the set of STOC-ML, STOC-NS and the one-way connection method to a full-scale case, where the 1868 Meiji-Sanriku tsunami attacks Kamaishi Port, Japan. Figure 4 shows the bathymetry of Kamaishi Port protected by two breakwaters, B1 and B2, between which a submerged breakwater is sandwiched. The bird's eye view of the breakwaters is briefly shown in Fig. 5. The tsunami is generated in STOC-ML, whose number of levels is one, by use of the seismic deformation model (Mansinha and Smylie, 1971) with fault parameters including length 210km, width 50km, depth 1km, dislocation 12.5m, slip 58 degrees, dip 20 degrees and strike 156 degrees (Sato ed., 1997), and correction coefficient of dislocation 0.75.

The area covered by STOC-NS is indicated in Fig. 4 as a one-kilometer square around the open mouth of tsunami breakwaters. This 3D calculation area, where horizontal mesh size is equally 12.5m, while vertical mesh size is variable from 1m to 10m, has built-in the connection area overlapping the STOC-ML's area from each side of the 3D calculation area towards its center by 10 meshes.

Calculation was conducted under nonslip condition on every wall and bottom, as mentioned above.

4.2 Calculation results and discussions

4.2.1 Water surface elevation

Water surface elevation at Point A in Fig. 4, over the center of the submerged breakwater, is shown in Fig. 6, where the solid line indicates the result given by the calculation with only STOC-ML whose number of levels is one, namely, a one-layer model, while the circles show the correspondent result obtained by STOC-NS with the one-way connection method after applying STOC-ML. The first peak of water surface elevation passes the center of submerged breakwater when t = 28.4min in both these cases. The two results are almost consistent except about the bottoms of trough. In the present paper we focus attention on the first period of tsunami.

4.2.2 Velocity distribution

Figure 7 shows velocity pattern in the vertical section including C-C' line inside the 3D calculation area drawn in Fig. 4. At this time, when the water surface displacement changes from negative to positive, the flow is

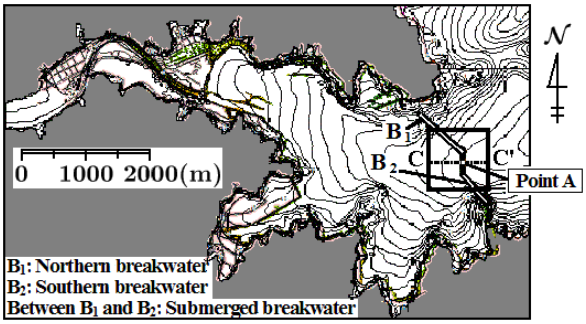

Figure 4. Plan view of Kamaishi Port, Japan.

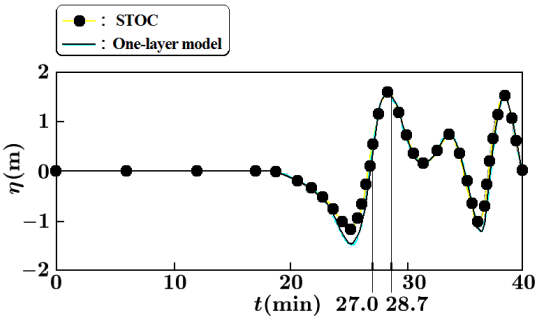

Figure 6. Water surface elevation at Point A.

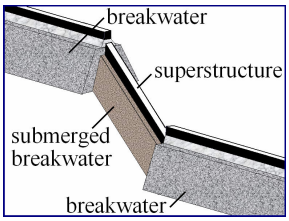

Figure 5. Sketch of breakwaters.

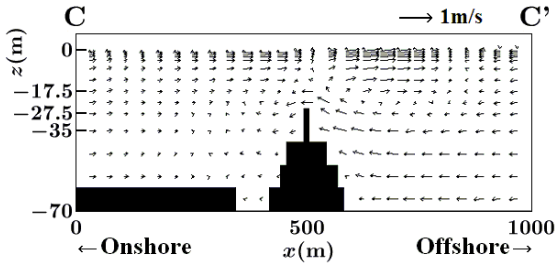

Figure 7. Velocity vectors in C-C' section (t = 27.0min).

dammed in front of the breakwater and raised over the submerged breakwater but under the offshore stream driven by the first draw-down.

On the other hand, Fig. 8 shows velocity patterns in the horizontal sections when t = 28.7min, showing influx behind the breakwaters, such that remarkably three-dimensional flow with both vertical and horizontal circulations are observed around the open mouth of breakwaters.

Thus STOC can provide three-dimensional fluid motion, which is a blue rose for one-layer long wave models.

4.2.3 Pressure on superstructure of submerged breakwater

The submerged breakwater, see Fig. 5, has its superstructure, on which tsunami force integrated spatially over this superstructure shows the maximum value when t = 28.7min, just after the peak time of water displacement. The calculation result of total pressure on this superstructure is shown in Fig. 9, where z = –27.5m and t = 28.7min. Difference between onshore-side pressure, p_{on}, and offshore-side pressure, p_{off}, in the direction perpendicular to the superstructure sides, i.e., $\Delta p = p_{off} - p_{on}$, works as net pressure on the structure.

Distribution of water level over the submerged breakwater at the same time is shown in Fig. 10, from which we obtain distribution of hydrostatic pressure. Accordingly we can evaluate the dynamic pressure determined as an excess over hydrostatic pressure, that is, the total pressure is a sum of hydrostatic and dynamic pressures. Figure 11 shows the net dynamic pressure, i.e., $\Delta p' = p_{off}' - p_{on}'$, indicating 1.35×10^4Pa at the center of the submerged breakwater where z = –27.5m, which accounts for about 58 percent of the net total pressure. Thus STOC can provide three-dimensional distribution of tsunami force on structures not just considering hydrostatic pressure but taking into account dynamic pressure as well, which is advantage of application of STOC-NS without assumption of hydrostatic pressure.

5 CONCLUSIONS

The numerical simulator, STOC, which consists of STOC-NS, STOC-ML and the connection model, has been developed to describe seawater motion from offshore to coastal zones due to tsunamis or storm surges

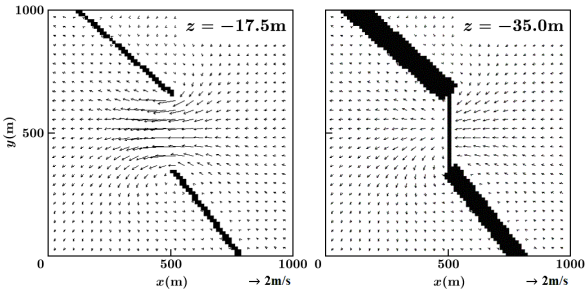

(a) $z = -17.5$m. (b) $z = -35.0$m.

Figure 8. Velocity vectors in horizontal sections (t = 28.7min).

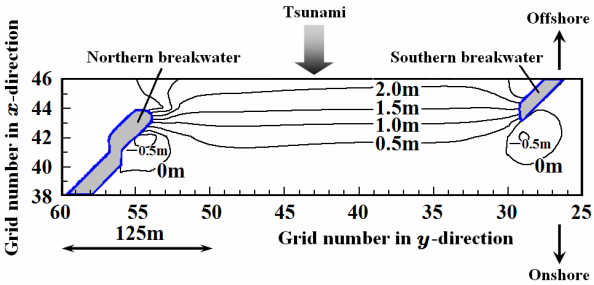

Figure 10. Distribution of water level around open mouth of breakwaters (t = 28.7min).

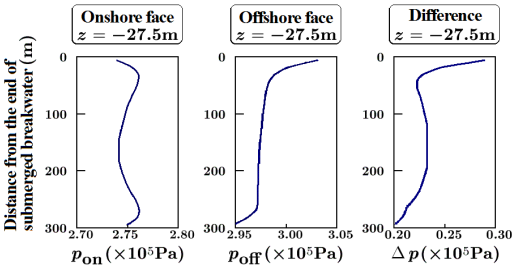

Figure 9. Total pressures on onshore and offshore faces of superstructure and net total pressures on superstructure of submerged breakwater (z = −27.5m, t = 28.7min, $\Delta p = p_{off} - p_{on}$).

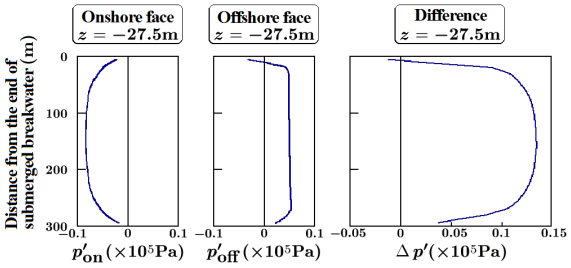

Figure 11. Dynamic pressures on onshore and offshore faces of superstructure and net dynamic pressures on superstructure of submerged breakwater (z = −27.5m, t = 28.7min, $\Delta p' = p_{off}' - p_{on}'$).

including inundation onto beaches. In comparison with theoretical, experimental and numerical data, the calculation results show accuracy of STOC in the various test cases.

In the present paper STOC was applied to tsunami calculation to represent the three-dimensional phenomena around the open mouth of tsunami breakwaters. We found the net dynamic pressure making up more than half of the net total pressure on the superstructure of submerged breakwater. STOC, which can provide three-dimensional distribution of fluid force on structures including not only hydrostatic but also dynamic pressures, has an edge on traditional long wave models based upon the assumption of hydrostatic pressure.

6 ACKNOWLEDGMENTS

Sincere gratitude is extended to Mr. M. Akiyama and Mr. A. Shimada, Fuji Research Institute Corporation, for beneficial help to program coding.

7 REFERENCES

Mansinha, L., and Smylie, D.E. (1971). "The Displacement Fields of Inclined Faults." *Bulletin of the Seismological Society of America*, Vol. 61, No. 5, pp. 1433-1440.

Masamura, K., Fujima, K., Goto, C., Iida, K., and Shigemura, T. (2001). "Numerical Analysis of Tsunami by Using 2D/3D Hybrid Model." *Journal of Hydraulics, Coastal and Environmental Engineering*, 670/II-54, pp. 49-61. (in Japanese)

Sakakiyama, T., and Kajima, R. (1992). "Numerical Simulation of Nonlinear Wave Interacting with Permeable Breakwaters." *Proceedings of 23rd International Conference on Coastal Engineering*, pp. 1517-1530.

Sato, Y. ed. (1997). *Handbook of Earthquake Dislocation Parameters in Japan*. Kajima Institute Publishing Co., Ltd., Tokyo, No. 52. (in Japanese)